JOURNAL OF AGRICULTURAL AND FOOD CHEMISTRY

Article

Identification and quantification of potential anti-inflammatory hydroxycinnamic acid amides from Wolfberries, fruits of Lycium barbarum

Siyu Wang, Joonhyuk Suh, Xi Zheng, Yu Wang, and Chi-Tang Ho

J. Agric. Food Chem., **Just Accepted Manuscript** • DOI: 10.1021/acs.jafc.6b05136 • Publication Date (Web): 23 Dec 2016

Just Accepted

ACS Publications

Journal of Agricultural and Food Chemistry is published by the American Chemical Society. 1155 Sixteenth Street N.W., Washington, DC 20036

Identification and quantification of potential anti-inflammatory hydroxycinnamic acid amides from Wolfberry

Siyu Wang,[†] Joon Hyuk Suh,[§] Xi Zheng,[&] Yu Wang,[§,*] and Chi-Tang Ho[†,*]

[†] Department of Food Science, Rutgers University, 65 Dudley Road, New Brunswick, NJ 08901, USA
[§] Food Science and Human Nutrition, Citrus Research and Education Center, University of Florida, 700 Experiment Station Rd, Lake Alfred, FL 33850 USA
[&] Susan Lehman Cullman Laboratory for Cancer Research, Department of Chemical Biology, Ernest Mario School of Pharmacy, Rutgers University, 164 Frelinghuysen Rd., Piscataway, NJ 08854

[*] Corresponding authors:

Yu Wang, Tel: (863)-956-8673; Fax: (863)-956-4631; Email: yu.wang@ufl.edu;

Chi-Tang Ho, Tel: (848)-932-5553; Fax: (732)-932-6776; Email: ctho@sebs.rutgers.edu

Abstract

Wolfberry or Goji berry, the fruit of *Lycium barbarum*, exhibits health-promoting properties that leads to an extensive study of their active components. We synthesized a set of hydroxycinnamic acid amide (HCCA) compounds, including *trans*-caffeic acid, *trans*-ferulic acid and 3,4-dihydroxyhydrocinnamic acid with extended phenolic amine components as standards to identify and quantify the corresponding compounds from wolfberry, and to investigate anti-inflammatory properties of these compounds using *in vitro* model. With optimized LC-MS/MS and NMR analysis, nine amide compounds were identified from the fruits. Seven of these compounds were identified in this plant for the first time. The amide compounds with a tyramine moiety were the most abundant. *In vitro* studies indicated that five HCCA compounds showed inhibitory effect on NO production inuded by LPS with IC_{50} less than 15.08 μM (*trans*-*N*-feruloyl dopamine). These findings suggested that wolfberries demonstrated anti-inflammatory properties.

Keywords: *Lycium Barbarum,* wolfberries, hydroxycinnamic acid amides, organic synthesis, anti-inflammation

Introduction

Hydroxycinnamic acid amides (HCAAs) are commonly found in flowering plants,[1] when cinnamate derivatives conjugate with either tyramine, tryptamine or dopamine derivatives.[2] . HCCAs play antibacterial and antiviral roles in plants as numerous studies strongly indicate certain amides contribute to plant defense mechanisms in response to microbial challenges and wound healing.[1-3] HCCA compounds, as secondary metabolites, are often considered as potential nutraceutical ingredients due to reports of health benefits such as anti-fungal,[4] antioxidant,[5] anti-inflammatory[6] as well as anti-cancer[7] properties.

The genus *Lycium* encompasses approximately 80 species unevenly distributed throughout South America, southern Africa, North America, Eurasia, Australia and several islands in the Pacific Ocean.[8] Wolfberry, the fruit of *Lycium barbarum*, is widely used in Asian cuisine. Recently, they have been marketed as dietary supplements and functional foods in multiple regions.[9] Their increase in popularity is due to numerous health benefits that improve kidney and liver function, immune system modulation, as well as provide anti-aging and cytoprotective effects.[10-11] The health benefits associated with wolfberry have led to investigations into isolating and identifying several categories of compounds, including polysaccharides,[12] polyphenols,[13-14] phenolic amides,[15] carotenoids,[16] flavonoids, organic acids and their derivatives.[17] Among these species, hydroxycinnamic acid derivatives are found to be abundant in this fruit[17]. By using preparative high performance liquid chromatography, Zhou et al. identified a set of dicaffeoylspermidine derivatives that provide effective antioxidant activities and protection against Alzheimer's disease.[15] Other bioactive HCCA compounds have been

identified from wolfberry. These include *cis*-*N*-feruloyltyramine, *trans*-*N*-feruloyltyramine and its dimer through the use of an activity-guided method and NMR-based identification.[18-19]

The anti-inflammatory properties of natural products have attracted more attention due to the large body of scientific evidence that supports the close relationship between chronic inflammation and many human diseases and conditions, as well as the potential health beneficial properties exerted by these food-sourced components.[20-21] Consequently, in addition to the antioxidant activities investigated in previous studies, some of these HCCA species identified from wolfberry have been shown to possess putative anti-inflammatory properties. For example, by following a bioactivity-guided method, *trans*-*N*-caffeoyltyramine was identified as an NF-κB inhibitor, which is known as a major transcription factor activated in response to inflammation and contributes to pro-inflammatory mediator production.[6] *trans*-*N*-feruloyltyramine was found to have an inhibitory effect on LPS-induced NO and prostaglandin E2 production through transcription factor AP-1 and the MAPK signaling pathway.[22]

The bioactive HCCA species identified from wolfberry lead to the hypothesis that there are potentially more HCCA species present in the fruit with possible anti-inflammatory properties. This prompted us to synthesize a series of amide compounds with similar extended amine components that potentially exist in wolfberry. In our investigation, we designed and synthesized three sets of HCCA compounds according to different hydroxycinnamic acid species, *trans*-caffeic acid, *trans*-ferulic acid and 3,4-dihydroxyhydrocinnamic acid. The objective was to use these synthetic amide compounds as references to identify and quantify compounds extracted from wolfberrry,

and further investigate their anti-inflammatory activities *in vitro.*

Materials and Method

Chemicals and reagents

trans-caffeic acid, *trans*-ferulic acid, 3,4-dihyroxyhydrocinnamic acid, phenethylamine, tryptamine, tyramine, dopamine hydrochloride, 3-phenylpropylamine, *N*-(3-dimethylaminopropyl)-*N*′-ethylcarbodiimide hydrochloride, sulfanilamide, naphthylethylenediamine dihydcrochloride, molecular biology grade dimethyl sulfoxide (DMSO), lipopolysaccharides (LPS) (*Escherichia coli* O127: E8), N^G-methyl-L-arginine acetate **(**L-NMMA) were purchased from Sigma-Aldrich (St. Louis, MO, USA). Triethylamine, 3,4-dimethoxyphenethylamine, LC-MS grade methanol, acetonitrile, water, and formic acid were purchased from Fisher Scientific (Fair Lawn, NJ, USA). Dimethylformamide (DMF), ethyl acetate, and hexane were purchased from Pharmco-AAPER (Brookfield, CT, USA). Gibco Dulbecco's Modified Eagle Medium (DMEM), fetal bovine serum (FBS), and streptomycin/penicillin solution were purchased from ThermoFisher Scientific (Hagerstown, MD, USA). Dimethyl sulfoxide-d_6 was purchased from Cambridge Isotope Laboratories, Inc. (Tewksbury, MA, USA)

General synthetic procedure

5 mM of hydroxycinnamic acid (*trans*-caffeic acid, *trans*-ferulic acid, or 3,4-dihydroxyhydrocinnamic acid) were mixed with 5 mM triethylamine in 10 mL DMF and placed on ice for 15 minutes. 7.5 mM of phenolic amine (phenethylamine, tryptamine, tyramine, 3-phenylpropylamine**,** dopamine hydrochloride or 3,4-dimethoxyphenethylamine) and 5 mM of *N*-(3-dimethylaminopropyl)-*N*′-ethylcarbodiimide hydrochloride were added to DMF under nitrogen atmosphere at room

temperature for 12 hours. The reaction solution was then mixed with 100 mL distilled water and extracted three times using 100 mL ethyl acetate. The organic layer was next washed with 0.2 M hydrochloric acid and brine, dried, evaporated and purified by using silica gel (standard grade, pore size 60 Å, 230-400 mesh particle size, 40-63 μm particle size) column chromatography (ethyl acetate and hexane), then finally freeze dried resulting in the target compounds. The purity of synthetic compounds was determined by TLC and NMR. The chemical structures of HCCA compounds are shown in Figure 1.

NMR analysis

Proton nuclear magnetic resonance spectra (^{1}H-NMR) were recorded on a Varian VNMRS-500 MHz, and Varian VNMRS 400 MHz instrument and reported in ppm using solvent containing TMS as an internal standard ($CDCl_3$ at 7.26 ppm, $(CD_3)_2SO$ at 2.50 ppm, CD_3OD at 3.31 ppm). Data are reported as s = singlet, d = doublet, t = triplet, dd = doublet of doublets, m = multiplet; integration; coupling constant(s) in Hz.

*N-trans-caffeoyl phenethylamine (**1**, Figure 1).* Yellow powder; HESIMS *m/z* 284.1 [M + H] (calcd for $C_{17}H_{17}NO_3$, 283.33); ^{1}H NMR (500 MHz, DMSO-d_6) δ 9.22 (d, J = 80.8 Hz, 2H), 8.04 (t, J = 5.7 Hz, 1H), 7.31−7.14 (m, 6H), 6.93 (d, J = 2.1 Hz, 1H), 6.81 (dd, J = 8.2, 2.1 Hz, 1H), 6.73 (d, J = 8.1 Hz, 1H), 6.31 (d, J = 15.7 Hz, 1H), 3.41−3.33 (m, 2H), 2.75 (t, J = 7.4 Hz, 2H). ^{13}C NMR (125 MHz, DMSO-d_6) δ 165.80, 147.70, 145.96, 139.97, 139.47, 129.06, 128.76, 126.82, 126.51, 120.82, 118.93, 116.18, 114.23, 40.76, 35.68.

*N-trans-caffeoyl 3,4-dimethoxyphenethylamine (**2,** Figure 1).* Yellow powder; HESIMS *m/z* 344.1 [M + H] (calcd for $C_{19}H_{21}NO_5$, 343.38); ^{1}H NMR (500 MHz, DMSO-d_6) δ 9.20 (s, 2H), 7.99 (t, *J* = 5.7 Hz, 1H), 7.21 (d, *J* = 15.6 Hz, 1H), 6.91 (d, *J* = 2.1 Hz, 1H), 6.84 (d, *J* = 8.2 Hz, 1H), 6.81–6.79 (m, 2H), 6.73–6.69 (m, 2H), 6.31 (d, *J* = 15.7 Hz, 1H), 3.71 (s, 3H), 3.69 (s, 3H), 3.37–3.33 (m, 2H), 2.67 (t, *J* = 7.3 Hz, 2H). ^{13}C NMR (125 MHz, DMSO-d_6) δ 165.76, 149.03, 147.68, 147.65, 145.95, 139.40, 132.40, 126.83, 120.87, 120.79, 118.99, 116.17, 114.21, 112.97, 112.33, 55.95, 55.80, 40.90, 35.21.

*N-trans-caffeoyl tryptamine (**3,** Figure 1).* Dark Yellow powder; HESIMS *m/z* 321.1 [M - H] (calcd for $C_{19}H_{18}N_2O_3$, 322.36); ^{1}H NMR (500 MHz, DMSO-d_6) δ 10.78 (s, 1H), 9.32 (s, 1H), 9.09 (s, 1H), 8.07 (t, *J* = 5.8 Hz, 1H), 7.54 (d, *J* = 7.9 Hz, 1H), 7.33 (s, 1H), 7.23 (d, *J* = 15.7 Hz, 1H), 7.14 (d, *J* = 2.3 Hz, 1H), 7.08−7.01 (m, 1H), 6.99−6.92 (m, 1H), 6.93 (d, *J* = 2.1 Hz, 1H), 6.82 (dd, *J* = 8.2, 2.0 Hz, 1H), 6.73 (d, *J* = 8.1 Hz, 1H), 6.32 (d, J = 15.7 Hz, 1H), 3.48−3.39 (m, 2H), 2.86 (t, *J* = 7.4 Hz, 2H). ^{13}C NMR (125 MHz, DMSO-d_6) δ 165.79, 147.66, 145.95, 139.37, 136.68, 127.67, 126.88, 123.06, 121.34, 120.77, 119.12, 118.71, 118.65, 116.17, 114.24, 112.30, 111.79, 40.02, 25.77.

*N-trans-caffeoyl tyramine (**4,** Figure 1).* Yellow powder; HESIMS *m/z* 300.1 [M + H] (calcd for $C_{17}H_{17}NO_4$, 299.33); ^{1}H NMR (500 MHz, DMSO-d_6) δ 9.31 (s, 1H), 9.14 (s, 1H), 9.08 (s, 1H), 7.98 (t, *J* = 5.7 Hz, 1H), 7.20 (d, *J* = 15.6 Hz, 1H), 6.99 (d, *J* = 8.4 Hz, 2H), 6.91 (d, *J* = 2.1 Hz, 1H), 6.80 (dd, *J* = 8.2, 2.1 Hz, 1H), 6.72 (d, *J* = 8.1 Hz, 1H), 6.66 (d, *J* = 8.3 Hz, 2H), 6.29 (d, *J* = 15.7 Hz, 1H), 3.32–3.25 (m, 2H), 2.62 (t, *J* = 7.4

Hz, 2H). ^{13}C NMR (125 MHz, DMSO-d_6) δ 165.72, 156.06, 147.67, 145.95, 139.37, 129.98, 129.90, 126.84, 120.79, 119.01, 116.17, 115.54, 114.23, 41.12, 34.90.

*N-trans-caffeoyl dopamine (**5,** Figure 1).* Yellow powder; HESIMS *m/z* 316.1 [M + H] (calcd for $C_{17}H_{17}NO_5$, 315.33); ^{1}H NMR (500 MHz, DMSO-d_6) δ 8.92 (s, 4H), 7.98 (t, *J* = 5.7 Hz, 1H), 7.21 (d, *J* = 15.7 Hz, 1H), 6.92 (d, *J* = 2.0 Hz, 1H), 6.81 (dd, *J* = 8.2, 2.1 Hz, 1H), 6.72 (d, *J* = 8.1 Hz, 1H), 6.62 (d, *J* = 7.9 Hz, 1H), 6.58 (d, *J* = 2.0 Hz, 1H), 6.43 (dd, *J* = 8.0, 2.1 Hz,1H), 6.30 (d, *J* = 15.6 Hz, 1H), 3.28 (dd, *J* = 14.0, 6.5 Hz, 2H), 2.59–2.52 (m, 2H). ^{13}C NMR (125 MHz, DMSO) δ 165.73, 147.67, 145.95, 145.48, 143.95, 139.37, 130.70, 126.85, 120.79, 119.65, 119.04, 116.41, 116.18, 115.93, 114.23, 41.16, 35.19.

*N-trans-feruloyl phenethylamine (**6,** Figure 1).* Colorless powder; HESIMS *m/z* 298.1 [M + H] (calcd for $C_{18}H_{19}NO_3$, 297.35); ^{1}H NMR (500 MHz, DMSO-d_6) δ 9.39 (s, 1H), 8.01 (t, *J* = 5.6 Hz, 1H), 7.34–7.24 (m, 3H), 7.24–7.16 (m, 3H), 7.12–7.07 (m, 1H), 6.96 (dd, *J* = 8.0, 1.9 Hz, 1H), 6.77 (dd, *J* = 8.0, 0.8 Hz, 1H), 6.42 (dd, *J* = 15.6, 0.8 Hz, 1H), 3.78 (s, 3H), 3.44–3.28 (m, 2H), 2.75 (t, *J* = 7.3 Hz, 2H). ^{13}C NMR (125 MHz, DMSO-d_6) δ 165.78, 148.68, 148.24, 139.95, 139.35, 129.05, 128.75, 126.84, 126.50, 121.94, 119.39, 116.07, 111.19, 55.95, 40.73, 35.66.

*N-trans-feruloyl 3,4-dimethoxyphenethylamine (**7,** Figure 1).* Colorless powder; HESIMS *m/z* 358.2 [M + H] (calcd for $C_{20}H_{23}NO_5$, 357.41); ^{1}H NMR (500 MHz, DMSO-d_6) δ 9.39 (s, 1H), 7.96 (t, *J* = 5.7 Hz, 1H), 7.30 (d, *J* = 15.6 Hz, 1H), 7.09 (d, *J* = 1.9 Hz, 1H),

6.96 (dd, J = 8.3, 1.9 Hz, 1H), 6.83 (d, J = 8.2 Hz, 1H), 6.80 (d, J = 2.0 Hz, 1H), 6.77 (d, J = 8.1 Hz, 1H), 6.71 (dd, J = 8.1, 2.0 Hz, 1H), 6.43 (d, J = 15.7 Hz, 1H), 3.78 (s, 3H), 3.72 (s, 3H), 3.69 (s, 3H), 3.43−3.34 (m, 2H), 2.68 (t, J = 7.3 Hz, 2H). ^{13}C NMR (125 MHz, DMSO-d_6) δ 165.76, 149.04, 148.66, 148.24, 147.65, 139.31, 132.36, 126.86, 121.91, 120.86, 119.45, 116.08, 112.95, 112.32, 111.18, 55.95, 55.93, 55.80, 40.86, 35.19.

*N-trans-feruloyl tryptamine (**8,** Figure 1).* Pale yellow powder; HESIMS *m/z* 337.2 [M + H] (calcd for $C_{20}H_{20}N_2O_3$, 336.39); ^{1}H NMR (500 MHz, DMSO-d_6) δ 10.80 (s, 1H), 9.39 (s, 1H), 8.04 (t, J = 5.7 Hz, 1H), 7.54 (d, J = 8.0 Hz, 1H), 7.35−7.32 (m, 2H), 7.16 (d, J = 2.0 Hz, 1H), 7.11 (d, J = 2.0 Hz, 1H), 7.05 (ddd, J = 8.1, 7.0, 1.2 Hz, 1H), 6.99−6.94 (m, 2H), 6.78 (d, J = 8.1 Hz, 1H), 6.45 (d, J = 15.7 Hz, 1H), 3.79 (s, 3H), 3.46 (dd, J = 13.1, 7.3 Hz, 2H), 2.87 (t, J = 6.9 Hz, 2H). ^{13}C NMR (125 MHz, DMSO-d_6) δ 165.79, 148.65, 148.25, 139.28, 136.70, 127.68, 126.91, 123.07, 121.93, 121.36, 119.60, 118.72, 118.66, 116.09, 112.28, 111.80, 111.19, 55.96, 39.99, 25.75.

*N-trans-feruloyl tyramine (**9,** Figure 1).* Colorless powder; HESIMS *m/z* 314.1 [M + H] (calcd for $C_{18}H_{19}NO_4$, 313.35); ^{1}H NMR (500 MHz, DMSO-d_6) δ 9.38 (s, 1H), 9.14 (s, 1H), 7.95 (t, J = 5.7 Hz, 1H), 7.29 (d, J = 15.7 Hz, 1H), 7.09 (d, J = 2.0 Hz, 1H), 6.99 (d, J = 8.4 Hz, 2H), 6.96 (dd, J = 8.2, 2.0 Hz, 1H), 6.77 (d, J = 8.1 Hz, 1H), 6.66 (d, J = 8.4 Hz, 2H), 6.41 (d, J = 15.8 Hz, 1H), 3.78 (s, 3H), 3.33−3.29 (m, 2H), 2.63 (t, J = 7.4 Hz, 2H). ^{13}C NMR (125 MHz, DMSO-d_6) δ 165.72, 156.06, 148.64, 148.23, 139.27, 129.95, 129.89, 126.86, 121.92, 119.47, 116.07, 115.54, 111.17, 55.95, 41.09, 34.87.

179

180 *N-trans-feruloyl 3-methoxytyramine (**10,** Figure 1).* Colorless powder; HESIMS *m/z*

181 344.2 [M + H] (calcd for $C_{19}H_{21}NO_5$, 343.38); ^{1}H NMR (500 MHz, DMSO-d_6) δ 9.38 (s,

182 1H), 8.68 (s, 1H), 7.95 (t, *J* = 5.7 Hz, 1H), 7.29 (d, *J* = 15.7 Hz, 1H), 7.09 (d, *J* = 1.9 Hz,

183 1H), 6.96 (dd, *J* = 8.3, 1.9 Hz, 1H), 6.80−6.73 (m, 2H), 6.66 (d, *J* = 8.0 Hz, 1H), 6.58 (dd,

184 *J* = 8.0, 1.9 Hz, 1H), 6.42 (d, *J* = 15.7 Hz, 1H), 3.78 (s, 3H), 3.72 (s, 3H), 3.38 - 3.29 (m,

185 2H), 2.64 (t, *J* = 7.4 Hz, 2H). ^{13}C NMR (125 MHz, DMSO-d_6) δ 165.73, 148.64, 148.24,

186 147.82, 145.22, 139.27, 130.65, 126.86, 121.90, 121.16, 119.49, 116.08, 115.77, 113.20,

187 111.17, 55.95, 55.94, 40.98, 35.24.

188

189 *N-trans-feruloyl dopamine (**11,** Figure 1).* Colorless powder; HESIMS *m/z* 330.1 [M + H]

190 (calcd for $C_{18}H_{19}NO_5$, 329.35); ^{1}H NMR (500 MHz, DMSO-d_6) δ 9.38 (s, 1H), 8.72 (s,

191 1H), 8.62 (s, 1H), 7.94 (t, *J* = 5.6 Hz, 1H), 7.29 (d, *J* = 15.7 Hz, 1H), 7.09 (d, *J* = 2.0 Hz,

192 1H), 6.96 (dd, *J* = 8.3, 1.9 Hz, 1H), 6.77 (d, *J* = 8.1 Hz, 1H), 6.62 (d, *J* = 7.9 Hz, 1H),

193 6.58 (d, *J* = 2.1 Hz, 1H), 6.48 - 6.35 (m, 2H), 3.78 (s, 3H), 3.33−3.23 (m, 2H), 2.56 (t, *J* =

194 7.4 Hz, 2H). ^{13}C NMR (125 MHz, DMSO-d_6) δ 165.70, 148.64, 148.23, 145.48, 143.95,

195 139.26, 130.68, 126.87, 121.92, 119.64, 119.50, 116.41, 116.07, 115.93, 111.17, 55.95,

196 41.12, 35.15.

197

198 *N-3,4-Dihydroxyhydrocinnamoyl phenethylamine (**12,** Figure 1).* Colorless liquid;

199 HESIMS *m/z* 286.1 [M + H] (calcd for $C_{17}H_{19}NO_3$, 285.34); ^{1}H NMR (500 MHz, DMSO-

200 d_6) δ 8.63 (s, 1H), 7.84 (t, *J* = 5.5 Hz, 1H), 7.29−7.21 (m, 2H), 7.17 (dt, *J* = 8.2, 1.8 Hz,

201 2H), 7.16−7.12 (m, 2H), 6.61−6.57 (m, 1H), 6.55 (d, *J* = 2.1 Hz, 1H), 6.40 (dd, *J* = 8.0,

2.2 Hz, 1H), 3.27−3.18 (m, 2H), 2.67−2.63 (m, 2H), 2.59 (t, J = 7.7 Hz, 2H), 2.24 (dd, J = 8.7, 6.9 Hz, 2H). ^{13}C NMR (125 MHz, DMSO-d_6) δ 171.85, 145.40, 143.72, 139.98, 132.60, 129.06, 128.71, 126.43, 119.16, 116.10, 115.82, 40.63, 38.00, 35.66, 31.04.

*N-3,4-Dihydroxyhydrocinnamoyl 3,4-dimethoxyphenthylamine (**13,** Figure 1).* Yellow amorphous powder; HESIMS *m/z* 346.2 [M + H] (calcd for $C_{19}H_{23}NO_5$, 345.40); ^{1}H NMR (500 MHz, DMSO-d_6) δ 8.69 (s, 1H), 8.59 (s, 1H), 7.81 (t, J = 5.6 Hz, 1H), 6.82 (d, J = 8.1 Hz, 1H), 6.75 (d, J = 2.0 Hz, 1H), 6.64 (dd, J = 8.2, 2.0 Hz, 1H), 6.60 (d, J = 8.0 Hz, 1H), 6.56 (d, J = 2.1 Hz, 1H), 6.40 (dd, J = 8.0, 2.1 Hz, 1H), 3.71 (s, 3H), 3.69 (s, 3H), 3.21 (dt, J = 7.7, 6.2 Hz, 2H), 2.62–2.58 (m, 4H), 2.28−2.21 (m, 2H).^{13}C NMR (125 MHz, DMSO-d_6) δ 172.35, 149.53, 145.92, 144.24, 133.15, 132.97, 121.41, 121.39, 119.67, 116.61, 116.35, 113.44, 112.84, 56.46, 56.30, 41.32, 38.53, 35.74, 31.59.

*N-3,4-Dihydroxyhydrocinnamoyl tryptamine (**14,** Figure 1).* Yellow amorphous powder; HESIMS *m/z* 325.2 [M + H] (calcd for $C_{19}H_{20}N_2O_3$, 324.38); ^{1}H NMR (500 MHz, DMSO-d_6) δ 10.76 (s, 1H), 8.63 (s, 2H), 7.88 (t, J = 5.8 Hz, 1H), 7.51 (d, J = 7.9 Hz, 1H), 7.31 (d, J = 8.1 Hz, 1H), 7.10 (s, 1H), 7.06−7.02 (m, 1H), 6.96 (t, J = 7.4 Hz, 1H), 6.60 (d, J = 7.9 Hz, 1H), 6.57 (d, J = 2.1 Hz, 1H), 6.41 (dd, J = 8.0, 2.1 Hz, 1H), 3.30 (dd, J = 13.8, 7.0 Hz, 2H), 2.77 (t, J = 7.5 Hz, 2H), 2.61 (dd, J = 8.9, 6.8 Hz, 2H), 2.30−2.21 (m, 2H). ^{13}C NMR (125 MHz, DMSO-d_6) δ 172.30, 145.90, 144.20, 137.15, 133.18, 128.17, 123.50, 121.80, 119.65, 119.18, 119.12, 116.59, 116.33, 112.83, 112.26, 40.42, 38.61, 31.57, 26.21.

*N-3,4-Dihydroxyhydrocinnamoyl tyramine (**15,** Figure 1).* Colorless amorphous powder; HESIMS *m/z* 302.1 [M + H] (calcd for $C_{17}H_{19}NO_4$, 301.34); ^{1}H NMR (500 MHz, DMSO-d_6) δ 8.88 (d, *J* = 153.8 Hz, 3H), 7.80 (t, *J* = 5.6 Hz, 1H), 6.95 - 6.91 (m, 2H), 6.67 - 6.63 (m, 2H), 6.60 (d, *J* = 8.0 Hz, 1H), 6.56 (d, *J* = 2.1 Hz, 1H), 6.40 (dd, *J* = 8.0, 2.1 Hz, 1H), 3.20–3.12 (m, 2H), 2.63–2.56 (m, 2H), 2.57–2.50 (m, 2H), 2.27–2.20 (m, 2H). ^{13}C NMR (125 MHz, DMSO-d_6) δ 171.81, 156.01, 145.40, 143.71, 132.63, 130.01, 129.90, 119.16, 116.10, 115.83, 115.51, 41.01, 38.02, 34.89, 31.06.

*N-3,4-Dihydroxyhydrocinnamoyl dopamine (**16,** Figure 1).* Colorless liquid; HESIMS *m/z* 318.2 [M + H] (calcd for $C_{17}H_{19}NO_5$, 317.34); ^{1}H NMR (500 MHz, DMSO-d_6) δ 8.63 (s, 4H), 7.79 (t, *J* = 5.6 Hz, 1H), 6.63 - 6.56 (m, 2H), 6.55 (d, *J* = 2.1 Hz, 2H), 6.39 (ddd, *J* = 8.1, 6.0, 2.1 Hz, 2H), 3.15–3.11 (m, 2H), 2.61−2.57 (m, 2H), 2.48−2.45 (m, 2H), 2.25−2.21 (m, 2H).^{13}C NMR (125 MHz, DMSO-d_6) δ 171.76, 145.46, 145.39, 143.91, 143.69, 132.65, 130.71, 119.64, 119.14, 116.37, 116.07, 115.89, 115.83, 41.02, 38.06, 35.19, 31.08.

*N-trans-feruloyl 3-phenylpropylamine (**17,** Figure 1).* Yellow liquid; HESIMS *m/z* 312.1 [M + H] (calcd for $C_{19}H_{21}NO_3$, 311.38); ^{1}H NMR (500 MHz, DMSO-d_6) δ 9.39 (s, 1H), 7.99 (t, *J* = 5.7 Hz, 1H), 7.32 (d, *J* = 15.7 Hz, 1H), 7.28–7.24 (m, 2H), 7.21–7.17 (m, 2H), 7.17–7.13 (m, 1H), 7.11 (d, *J* = 2.0 Hz, 1H), 6.97 (dd, *J* = 8.2, 1.9 Hz, 1H), 6.78 (d, *J* = 8.1 Hz, 1H), 6.44 (d, *J* = 15.7 Hz, 1H), 3.79 (s, 3H), 3.20–3.09 (m, 2H), 2.63 - 2.54 (m, 2H), 1.78 - 1.68 (m, 2H). ^{13}C NMR (125 MHz, DMSO-d_6) δ 166.26, 149.14, 148.74,

142.63, 139.77, 129.23, 129.20, 129.17, 127.37, 126.65, 122.43, 119.97, 116.57, 111.63, 56.43, 39.21, 33.52, 31.95, 15.01.

LC-MS/MS analysis

LC separation was performed with an Ultimate 3000 system (Dionex, Sunnyvale, CA, USA) including an RS pump, an XRS Open autosampler, and an RS column compartment. Sixteen amide compounds were simultaneously chromatographed on a Synergi Fusion-RP column (2.0 mm × 100 mm, 2.5 μm particle size, Phenomenex, Torrance, CA, USA). The column temperature was set to 25 °C. Gradient elution of mobile phase A (0.1% formic acid in water) and B (0.1% formic acid in acetonitrile) was applied with a flow rate of 0.4 mL/min with a linear gradient from 20% to 100% solvent B for 0-5 min, holding at 100% solvent B for 5-7 min, and then returning to 20% solvent B for column equilibration. The injection volume was 10 μL.

MS detection was conducted on a triple quadrupole mass spectrometer (TSQ Quantiva, Thermo Fisher Scientific, San Jose, CA, USA) with selected reaction monitoring (SRM). The instrument was operated with a heated-electrospray ionization (HESI) in both polarity modes. All compounds except for compound **3** were analyzed in positive mode, and only compound **3** was detected in negative mode. Nitrogen gas was used as both sheath and auxiliary gas. Argon gas was employed as the collision gas. The ion source conditions were as follows: positive spray voltage, 3,500 V; negative spray voltage, 2,500 V; sheath gas, 45 Arb; aux gas, 15 Arb; sweep gas, 1 Arb; ion transfer tube temperature, 350 °C; and vaporizer temperature, 350 °C. The MS/MS parameters were optimized as follows: collision gas pressure, 2 mTorr; source fragmentation voltage, 0 V;

chrom filter, 3 sec; and dwell time, 100 msec. RF lens voltage was 85 V for compound **3** and **10**, and was 65 V for the others. Data analysis was performed using Xcaliber software (Ver. 3.0).

Preparation of standard solutions

Stock solutions were prepared at a concentration of 1,000 μg/mL, filtered through 0.45 μm nylon membrane filters, and stored at -20 °C until use. **1**, **2**, **3**, **4**, **6**, **7**, **8** and **9** were dissolved in dimethyl sulfoxide, **12**, **13**, **14** and **15** were dissolved in dimethyl sulfoxide:methanol (1:1) mixture, and **5**, **10**, **11**, and **16** were dissolved in dimethyl sulfoxide:methanol (1:4) mixture. Standard working solutions were prepared by diluting and mixing each stock solution with methanol to obtain proper concentrations. For compound **17** (internal standard), a stock solution was prepared in dimethyl sulfoxide:methanol (1:4) mixture at a concentration at 1,000 μg/mL, and a working solution was prepared by diluting the stock solution with methanol. Each sample contained 10 ng/mL of internal standard.

Preparation of samples

Dried wolberries were finely ground into powder, and then extracted using one of two different methods. For compounds **9** and **10**, which were found in relatively high quantities in the sample, 10 mg of the powder was extracted using 4.5 mL of methanol and 0.5 mL of internal standard solution in an ultrasonic bath at ambient temperature for 40 min. After vigorous agitation by using a multi-tube vortexer for 1 h, the resultant solution was filtered through a 0.45 μm membrane filter, and injected into the LC-MS.

For all other compounds, an evaporation procedure was added during the extraction. 100 mg of the powder was extracted using 4.5 mL of methanol and 0.5 mL of internal standard solution using the same procedure previously described. Then, 3 mL of the filtrate was vaporized under nitrogen, and the residue was suspended in 0.3 mL of methanol before injection into the LC-MS/MS system.

Cell culture

RAW264.7 murine macrophages were purchased from the American Type Culture Collection (Manassas, VA, USA). Cells were cultured in high-glucose Dulbecco's Modified Eagle's medium, supplemented with 100 IU/mL penicillin/streptomycin, 1 mM sodium pyruvate and 10% fetal bovine serum. Cells were incubated in 10 cm culture Petri dishes in 5% CO_2 with 70% humidity at 37 °C.

Cell viability Assay

4×10^5 cells/mL were seeded into 96-well plates and incubated for 12 hours before treatment. Compounds of interest were first dissolved in molecular biology grade DMSO at a concentration of 100 μM, and were further diluted with growth media to reach the final assay concentration. Growth media with 0.01% v/v DMSO served as the control. 75 μg/mL of L-NMMA was used as a positive control. Either the compound of interest or a vehicle was added to the medium and then incubated for 24 hr. After treatment, cells were washed twice with phosphate buffered saline. Phenol red free medium containing 5 mg/mL of 3-(4,5-dimethylthiazol-2-yl)-2,5-diphenyltetrazolium bromide was added to

cells and then incubated at 37 °C for 4 hours. After removing the supernatant, formazan crystals were dissolved in 150 μL of DMSO. Optical densities were measured at 570 nm.

Nitrite Assay

100 μM DMSO stock solutions of test compounds were diluted with growth media to achieve assay concentrations.75 μg/mL L-NMMA was used as positive control. Cells (4×10^5 cells/mL) were treated with *E. coli* LPS (100 ng/mL) in either the presence of the compound of interest or 0.01% dimethyl sulfoxide (DMSO) as a vehicle in phenol red free medium for 24 hours. After a 12-hour incubation period, 50 μL of conditional supernatant was removed, mixed with an equal volume of Griess reagent (1% sulfanilamide in 5% phosphoric acid and 0.1% naphthylethylenediamine dihydrochloride in water), and incubated at room temperature for 10 minutes. Production of nitrite was measured at an absorbance of 550 nm.

Statistical Analysis

All compound quantification results are shown as mean ± standard deviation. Statistical analysis for IC_{50} was performed using Prism 7 by non-linear regression. IC_{50} values are shown as mean ± standard error. All experimental data were obtained independently and replicated a total of three times. Significant differences were determined as $p < 0.05$.

Results and discussion

NMR of synthetic amide compounds

Amide structures were confirmed using the triplet with coupling constant of *J* ~5.7 Hz. ^{1}H NMR spectrum of caffeoyl and feruloyl amides had two vinyl doublets with a coupling constant of *J* ~15.7 Hz, and feruloyl amides also had a methoxyl singlet at 3.80 ppm. 3,4-dihydroxyhydrocinnamoyl amides lost the vinyl structure and alternately, characteristic methylene chemical shifts around 2.58 ppm were found. 3,4-dimethoxylphenethylamine moieties had two singlets with a chemical shift of ~3.70 ppm, which were attributed to two methoxyl groups. An indole singlet above 10 ppm confirmed the tryptamine moieties in compounds **3**, **8**, and **14**.

Quantification of amide compounds

The LC-MS/MS analytical results showed that the fruits had amide compounds at various concentrations. For example, the content of **9** was greater than 10,000-fold more than that of **7**, whereas some compounds only presented in nanogram quantities.

The established LC-MS/MS method was applied to comprehensive analysis and quantitative evaluation of the fruits samples. The analysis was performed in triplicate (n=3). The chromatograms of 16 amide compounds are shown in Figure 2. The compounds were fairly well separated from interferences. The retention times of compounds **1**-**16** and **17** (internal standard) are 2.93 min, 2.66 min, 2.98 min, 2.32 min, 2.03 min, 3.25 min, 2.97 min, 3.25 min, 2.64 min, 2.36 min, 2.71 min, 2.46 min, 2.81 min, 2.04 min, 1.71 min, 2.68 min and 3.49 min, respectively. Quantification of each analyte in the samples was calculated using the ratio of peak area (analyte peak area

versus internal standard peak area) based on the calibration curve of each individual standard. The correlation coefficient values of all models exhibited good linearity (R^2 > 0.998) (Supplementary Figure 1). The results indicated successful application of the LC-MS/MS method for the quantification of amide compounds in different quantities. The major constituents in the fruits were found to be **4**, **5**, **9**, **10** and **11**. Their contents were between 107.2 and 11109.6 ng/g. The content of 3Tyra was 12.1 ng/g. All compounds contained a tyramine or dopamine moiety, whereas compounds, **6-8,** having a phenethylamine, 3,4-dimethoxyphenethylamine or tryptamine moiety, were found to be minor ones (0.7 to 3.1 ng/g). Table 1 lists the mean concentrations of amide compounds detected in the samples.

The methodology for identification of HCCA compounds from wolfberries

In our study, a novel identification method used synthetic standards as references for LC-MS/MS analysis that compensated for the drawbacks of identification and isolation of minor components from the plants. Our synthesis design was based on the results from literatures and plant biosynthesis pathway of HCCA compounds. HCCA compounds form a large class of secondary metabolites abundantly present in plants, serving as growth and floral signaling compounds as well as metabolic intermediates.[1, 23] In addition to the HCCA compounds isolated from the wolfberry fruits, several studies reported that HCCA compounds with *trans*-caffeic, *trans*-ferulic and 3,4-dihydroxyhydrocinnamic acid moieties were isolated from the root bark of the plant.[24, 25] These hydroxycinnamoyl moieties derived from deaminated phenylalanine, and these hydroxycinnamic acid precursors, including *trans*-caffeic acid and *trans*-ferulic acid were

also identified from wolfberries[17]. Thus, we proposed that HCCA compounds were synthesized from these three hydroxycinnamic acid families. Amine moieties could result from decarboxylated amino acid; for instance, *trans*-feruloyl tyramine is the most common HCCA species conjugated from decarboxylated amino acid, tyrosine, which was also found in wolfberry and other plant species.[26-28] Plant aromatic L-amino acid decarboxylases generate phenethylamine, tryptamine and dopamine conjugates from L-phenylalanine, L-tryptophan and L-Dopa, respectively.[29] The amine conjugates can be further modified through species-specific hydroxylation or methylation reaction,[30] which gives possible methoxylated species, in our case, 3,4-dimethoxyphenethylamine and 3-methoxytyramine. Finally, the coupling of hydrocycinnamoyl and amine moieties is catalyzed by a diverse set of specific hydroxycinnamoyl transferases.[30] As a result, we designed the synthesis from three hydroxycinnamic acid species with similar extended amine moieties.

As shown in Table 1, our method did improve sensitivities to identify minor components from the plants. We identified compounds **6**, **7**, **8** and **15** with concentrations as low as 0.7 ng/g. Furthermore, by using reference standards, LC-MS/MS analysis differentiated structural analogs with high sensitivities, which may remain a challenge using traditional identification and isolation processes.

Nitric Oxide inhibition of HCCAs

Chronic inflammation is a complex process mediated by activation of inflammatory or immune cells and has been shown to trigger chronic disorders. During the inflammatory response, macrophages play a critical role in managing inflammatory

405 phenomena such as the overproduction of pro-inflammatory cytokines and inflammatory
406 mediators, including nitric oxide (NO). In order to select proper concentrations of the
407 compounds of interest for the anti-inflammatory studies, murine macrophage RAW264.7
408 cells were treated with the compounds of interest at various concentrations or 0.01%
409 DMSO vehicle for 24 hours, and cell viability was determined by MTT assay. Among the
410 IC_{50} values shown in Table 2, all of the tested compounds possessed IC_{50} values larger
411 than 100 μM, indicating low cytotoxicity of these compounds, which was also shown in
412 Figure 3.

413 The NO production inhibitory effects of these HCCA compounds were
414 investigated by co-incubating RAW264.7 murine macrophages with the test HCCA
415 compounds and LPS (100 ng/mL) for 24 hours. The NO accumulation in cell medium
416 was measured by Griess reagent. After LPS stimulation, the NO production significantly
417 increased compared to the negative control groups, and could be observed in all
418 experimental groups, as seen in Figure 4. These results are shown in Table 2. A total of
419 five HCCA compounds exhibited NO inhibitory properties, including two HCCA
420 compounds with *trans*-caffeic acid moiety, compounds **4**, and **5**, two compounds with
421 *trans*-ferulic acid moiety, **6** and **11**, and one compound with 3,4-dihydrohydroxycinnamic
422 acid moiety, **15**. Compound **5** was found to be the most potent compound that inhibited
423 NO production in LPS-induced murine macrophage with the lowest IC_{50} value, followed
424 by **4**, which also showed significant inhibitory effects on NO production. Hence, in
425 wolfberry, these two compounds are abundantly present (Table 1).

426 These results suggest excellent anti-inflammatory properties of the HCCA
427 compounds, especially the caffeic acid derivatives. Further efforts have been proposed to

study the detailed structure-activity relationship of HCCA compounds and their anti-inflammatory effects, as well as the underlying anti-inflammatory mechanism.

In our study, 16 HCCA compounds that potentially exist in wolfberry were synthesized and used as reference standards for LC/MS-MS analysis. Among these candidates, nine amide compounds were identified from the fruits. Furthermore, seven of these compounds were identified for the first time in this plant (compounds **5**-**8**, **11**, **15**), and all the compounds found in the plant were directly quantified. By using HCCA species from wolfberry as a model, we proposed a methodology for natural products identification with improved sensitivities, which differentiate structural analogs as well as identify minor chemical components.

The anti-inflammatory activities of these compounds were investigated *in vitro* using an RAW264.7 cell model. We found that these compounds exhibited a promising inhibitory effect on NO production. Compounds **4** and **11** showed significant potency in NO inhibition. The major advantage of amide compounds is their stable characteristic at physicological condition, leading to broader applications. Future plans include elucidation of detailed molecular mechanisms of anti-inflammatory properties using both *in vitro* and *in vivo* models, as well as their absorption and metabolism. The discovery of novel HCCA compounds from worberry broadened the variety of this family in the plant, enhancing potential use of wolfberry as functional ingredients in foods and dietary supplements to prevent and treat of inflammation and inflammation-related diseases.

Funding

Researches fund by USDA NIFA Hatch Project NJ10136.

451

452 **Supporting Information**

453 The supporting information contains SRM parameter setting for compound **1**-**17** and LC-

454 MS/MS spectrum of compound **1**-**17**

455

References

1. Martin-Tanguy, J.; Cabanne, F.; Perdrizet, E.; Martin, C., The distribution of hydroxycinnamic acid amides in flowering plants. *Phytochemistry* **1978,** *17*, 1927-1928.

2. Facchini, P. J.; Hagel, J.; Zulak, K. G., Hydroxycinnamic acid amide metabolism: physiology and biochemistry. *Canadian Journal of Botany* **2002,** *80*, 577-589.

3. Campos, L.; Lisón, P.; López-Gresa, M. P.; Rodrigo, I.; Zacarés, L.; Conejero, V.; Bellés, J. M., Transgenic tomato plants overexpressing tyramine *N*-hydroxycinnamoyltransferase exhibit elevated hydroxycinnamic acid amide levels and enhanced resistance to *Pseudomonas syringae*. *Molecular Plant-Microbe Interactions* **2014,** *27*, 1159-1169.

4. Lee, D. G.; Park, Y.; Kim, M.-R.; Jung, H. J.; Seu, Y. B.; Hahm, K.-S.; Woo, E.-R., Anti-fungal effects of phenolic amides isolated from the root bark of *Lycium chinense*. *Biotechnol. Lett.* **2004,** *26*, 1125-1130.

5. Lee, Y.-T.; Hsieh, Y.-L.; Yeh, Y.-H.; Huang, C.-Y., Synthesis of phenolic amides and evaluation of their antioxidant and anti-inflammatory activity in vitro and *in vivo*. *RSC Adv.* **2015,** *5*, 85806-85815.

6. Xie, L. W.; Atanasov, A. G.; Guo, D. A.; Malainer, C.; Zhang, J. X.; Zehl, M.; Guan, S. H.; Heiss, E. H.; Urban, E.; Dirsch, V. M.; Kopp, B., Activity-guided isolation of NF-kappaB inhibitors and PPARgamma agonists from the root bark of Lycium chinense Miller. *J. Ethnopharmacol.* **2014,** *152*, 470-7.

7. Park, J. B.; Schoene, N., N-Caffeoyltyramine arrests growth of U937 and Jurkat cells by inhibiting protein tyrosine phosphorylation and inducing caspase-3. *Cancer Lett.* **2003,** *202*, 161-171.

8. Fukuda, T.; Yokoyama, J.; Ohashi, H., Phylogeny and biogeography of the genus Lycium (Solanaceae): inferences from chloroplast DNA sequences. *Mol. Phylogen. Evol.* **2001,** *19*, 246-258.

9. Amagase, H.; Farnsworth, N. R., A review of botanical characteristics, phytochemistry, clinical relevance in efficacy and safety of *Lycium barbarum* fruit (Goji). *Food Res. Int.* **2011,** *44*, 1702-1717.

10. Chang, R. C.-C.; So, K.-F., Use of anti-aging herbal medicine, Lycium barbarum, against aging-associated diseases. What do we know so far? *Cell. Mol. Neurobiol.* **2008,** *28*, 643-652.

11. Song, M.; Salam, N.; Roufogalis, B. D.; Huang, T., Lycium barbarum (Goji Berry) extracts and its taurine component inhibit PPAR-γ-dependent gene transcription in human retinal pigment epithelial cells: possible implications for diabetic retinopathy treatment. *Biochem. Pharmacol.* **2011,** *82*, 1209-1218.

12. Redgwell, R. J.; Curti, D.; Wang, J.; Dobruchowska, J. M.; Gerwig, G. J.; Kamerling, J. P.; Bucheli, P., Cell wall polysaccharides of Chinese wolfberry (*Lycium barbarum*): Part 2. Characterisation of arabinogalactan-proteins. *Carbohydr. Polym.* **2011,** *84*, 1075-1083.

13. Zhou, Z.-Q.; Xiao, J.; Fan, H.-X.; Yu, Y.; He, R.-R.; Feng, X.-L.; Kurihara, H.; So, K.-F.; Yao, X.-S.; Gao, H., Polyphenols from wolfberry and their bioactivities. *Food Chem.* **2017,** *214*, 644-654.

14. Le, K.; Chiu, F.; Ng, K., Identification and quantification of antioxidants in Fructus lycii. *Food Chem.* **2007,** *105*, 353-363.

15. Zhou, Z.-Q.; Fan, H.-X.; He, R.-R.; Xiao, J.; Tsoi, B.; Lan, K.-H.; Kurihara, H.; So, K.-F.; Yao, X.-S.; Gao, H., Lycibarbarspermidines A–O, new dicaffeoylspermidine derivatives from wolfberry, with activities against Alzheimer's disease and oxidation. *J. Agric. Food Chem.* **2016,** *64*, 2223-2237.

16. Peng, Y.; Ma, C.; Li, Y.; Leung, K. S.-Y.; Jiang, Z.-H.; Zhao, Z., Quantification of zeaxanthin dipalmitate and total carotenoids in Lycium fruits (*Fructus Lycii*). *Plant Foods Hum. Nutr.* **2005,** *60*, 161-164.

17. Inbaraj, B. S.; Lu, H.; Kao, T. H.; Chen, B. H., Simultaneous determination of phenolic acids and flavonoids in *Lycium barbarum* Linnaeus by HPLC–DAD–ESI-MS. *J. Pharm. Biomed. Anal.* **2010,** *51*, 549-556.

18. Forino, M.; Tartaglione, L.; Dell'Aversano, C.; Ciminiello, P., NMR-based identification of the phenolic profile of fruits of *Lycium barbarum* (goji berries). Isolation and structural determination of a novel N-feruloyl tyramine dimer as the most abundant antioxidant polyphenol of goji berries. *Food Chem.* **2016,** *194*, 1254-1259.

19. Gao, K.; Ma, D.; Cheng, Y.; Tian, X.; Lu, Y.; Du, X.; Tang, H.; Chen, J., Three new dimers and two monomers of phenolic amides from the fruits of *Lycium barbarum* and their antioxidant activities. *J. Agric. Food Chem.* **2015,** *63*, 1067-1075.

20. Pan, M.-H.; Lai, C.-S.; Ho, C.-T., Anti-inflammatory activity of natural dietary flavonoids. *Food Funct.* **2010,** *1*, 15-31.

21. Pan, M.-H.; Lai, C.-S.; Dushenkov, S.; Ho, C.-T., Modulation of inflammatory genes by natural dietary bioactive compounds. *J. Agric. Food Chem.* **2009,** *57*, 4467-4477.

22. Jiang, Y.; Yu, L.; Wang, M.-H., N-trans-feruloyltyramine inhibits LPS-induced NO and PGE 2 production in RAW 264.7 macrophages: Involvement of AP-1 and MAP kinase signalling pathways. *Chem.-Biol. Interact.* **2015,** *235*, 56-62.

23. Matsuno, M.; Compagnon, V.; Schoch, G. A.; Schmitt, M.; Debayle, D.; Bassard, J.-E.; Pollet, B.; Hehn, A.; Heintz, D.; Ullmann, P.; Lapierre, C.; Bernier, F.; Ehlting, J.; Werck-Reichhart, D., Evolution of a Novel Phenolic Pathway for Pollen Development. *Science* **2009,** *325*, 1688-1692.

24. Zhang, J. X.; Guan, S. H.; Yang, M.; Feng, R. H.; Wang, Y.; Zhang, Y. B.; Chen, X.; Chen, X. H.; Bi, K. S.; Guo, D. A., Simultaneous determination of 24 constituents in *Cortex Lycii* using high-performance liquid chromatography-triple quadrupole mass spectrometry. *J. Pharm. Biomed. Anal.* **2013,** *77*, 63-70.

25. Zhang, J.; Guan, S.; Sun, J.; Liu, T.; Chen, P.; Feng, R.; Chen, X.; Wu, W.; Yang, M.; Guo, D.-a., Characterization and profiling of phenolic amides from *Cortex Lycii* by ultra-high performance liquid chromatography coupled with LTQ-Orbitrap mass spectrometry. *Anal. Bioanal. Chem.* **2015,** *407*, 581-595.

26. Amaro, C.; González-Cortazar, M.; Herrera-Ruiz, M.; Román-Ramos, R.; Aguilar-Santamaría, L.; Tortoriello, J.; Jiménez-Ferrer, E., Hypoglycemic and hypotensive activity of a root extract of *Smilax aristolochiifolia*, standardized on *N-trans*-feruloyl-tyramine. *Molecules* **2014,** *19*, 11366-11384.

27. Yoshihara, T.; Takamatsu, S.; Sakamura, S., Three new phenolic amides from the roots of eggplant (*Solanum melongena* L.). *Agric. Biol. Chem.* **2014,** *42*, 623-627.

544 28. Yoshihara, T.; Yamaguchi, K.; Takamatsu, S.; Sakamura, S., A New lignan
545 amide, grossamide, from bell pepper (*Capsicum annuum* var. grossurri). *Agric. Biol.*
546 *Chem.* **2014,** *45*, 2593-2598.
547 29. Facchini, P. J.; Huber-Allanach, K. L.; Tari, L. W., Plant aromatic L-amino acid
548 decarboxylases- evolution, biochemistry, regulation, and metabolic engineering
549 applications. *Phytochemistry* **2000,** *54*, 121-138.
550 30. Bassard, J.-E.; Ullmann, P.; Bernier, F.; Werck-Reichhart, D., Phenolamides:
551 Bridging polyamines to the phenolic metabolism. *Phytochemistry* **2010,** *71*, 1808-1824.
552

553 **Figure Captions**

554 **Figure 1**. Chemical structure of HCCA synthetic compounds. Compounds **1-5** were
555 *trans*-caffeic acid species. Compounds **6-11** were *trans*-ferulic acid species, and
556 compounds **12-16** were 3,4-dihydroxyhydrocinnamic acid species. Compound **17** was
557 synthesized by *trans*-ferulic acid and 3-phenylpropylamine, and used as the internal
558 standard for quantification.

559

560 **Figure 2.** LC-MS/MS chromatograms of standards (A) and fruit extracts (B): **1** *N-trans*-
561 caffeoyl phenethylamine, **2** *N-trans*-caffeoyl 3,4-dimethoxyphenethylamine, **3** N-*trans*-
562 caffeoyl tryptamine, **4** *N-trans*-caffeoyl tyramine, **5** *N-trans*-caffeoyl dopamine, **6** *N-*
563 *trans*-feruloyl phenethylamine, **7** *N-trans*-feruloyl 3,4-dimethoxyphenethylamine, **8** *N-*
564 *trans*-feruloyl tryptamine, **9** *N-trans*-feruloyl tyramine, **10** *N-trans*-feruloyl 3-
565 methoxytyramine, **11** *N-trans*-feruloyl dopamine, **12** *N*-3,4-
566 Dihydroxyhydrocinnamoyl phenethylamine, **13** *N*-3,4-Dihydroxyhydrocinnamoyl 3,4-
567 dimethoxyphenethylamine, **14** *N*-3,4-Dihydroxyhydrocinnamoyl tryptamine, **15** *N-3,4-*
568 Dihydroxyhydrocinnamoyl tyramine, **16** *N*-3,4-Dihydroxyhydrocinnamoyl dopamine,
569 and **17** *N-trans*-feruloyl 3-phenylpropylamine (internal standard)

570

571 **Figure 3.** Cytotoxicity of HCCA compounds on RAW264.7 cells. 75 μg/mL L-NMMA
572 was used as a positive control. The cells were incubated with compounds of interest or
573 vehicle control (0.01% DMSO) for 24 hour. Asterisks indicate significant differences
574 from the control (0 μM) determined using Dunnett's multiple comparison t-test (*$p <$
575 0.05, ** $p < 0.005$, *** $p < 0.001$, **** $p < 0.0001$).

576

577 **Figure 4.** Effect of HCCA compounds on LPS-induced NO release of RAW624.7 cell. 75
578 μg/mL L-NMMA was used as the positive control. Compounds of interested were co-incu
579 bated with 100 ng/mL LPS for 24 hour. Negative control groups (-) were incubated with
580 growth media only without LPS or compounds of interest. The NO accumulation in cell
581 medium was measured by Griess reagent. Asterisks indicate significant differences from
582 the control (0 μM) determined using Dunnett's multiple comparison t-test (*$p < 0.05$, **
583 $p < 0.005$, *** $p < 0.001$, **** $p < 0.0001$).5

584

Table 1. Mean Concentrations of Amide Compounds in Wolfberry (n = 3).

Compound No.	Compound name	Mean ± Standard Error (ng/g)
4	*N-trans*-caffeoyl tyramine	237.6 ± 6.2
5	*N-trans*-caffeoyl dopamine	107.2 ± 2.3
6	*N-trans*-feruloyl phenethylamine	3.1 ± 0.1
7	*N-trans*-feruloyl 3,4-dimethoxyphenethylamine	0.9 ± 0.0
8	*N-trans*-feruloyl tryptamine	0.7 ± 0.0
9	*N-trans*-feruloyl tyramine	11110± 140
10	*N-trans*-feruloyl 3-methoxytyramine	634.4 ± 21.3
11	*N-trans*-feruloyl dopamine	516.6 ± 27.4
15	*N*-3,4-Dihydroxyhydrocinnamoyl tyramine	12.1 ± 0.3

Table 2. Cytotoxicity IC_{50} value and NO Production IC_{50} value of HCCA compounds to RAW 264.7.

Compd.	IC_{50} (Mean±Standard Error) μM	50% NO inhibition conc. (Mean± Standard Error) μM
4	>100 μM	12.76±1.66
5	>100 μM	39.05±3.53
6	>100 μM	14.28±2.10
7	>100 μM	>10 μM
8	>100 μM	>50 μM
9	>100 μM	>50 μM
10	>100 μM	>50 μM
11	>100 μM	15.08±0.80
15	>100 μM	40.36±4.65

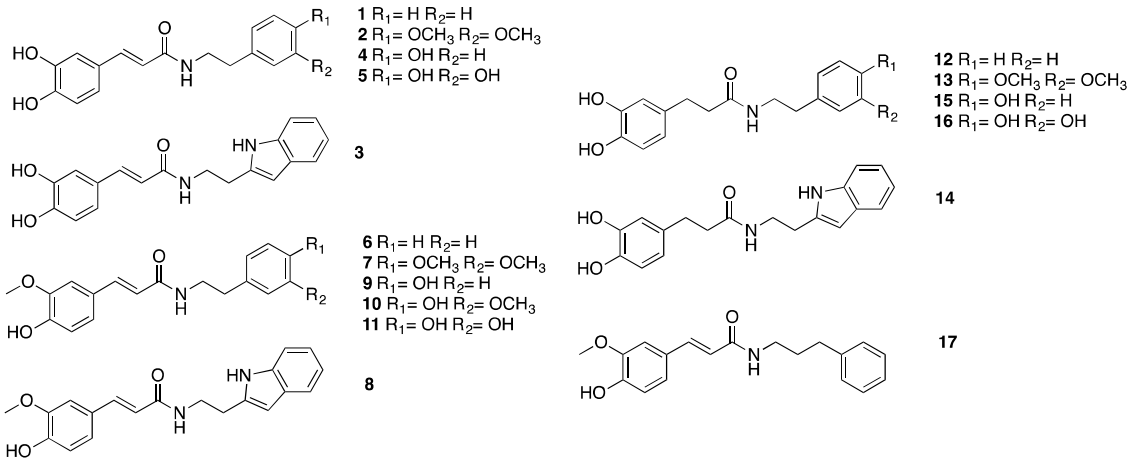
1 R1= H R2= H
2 R1= OCH3 R2= OCH3
4 R1= OH R2= H
5 R1= OH R2= OH
3
6 R1= H R2= H
7 R1= OCH3 R2= OCH3
9 R1= OH R2= H
10 R1= OH R2= OCH3
11 R1= OH R2= OH
8
12 R1= H R2= H
13 R1= OCH3 R2= OCH3
15 R1= OH R2= H
16 R1= OH R2= OH
14
17

Figure 1.

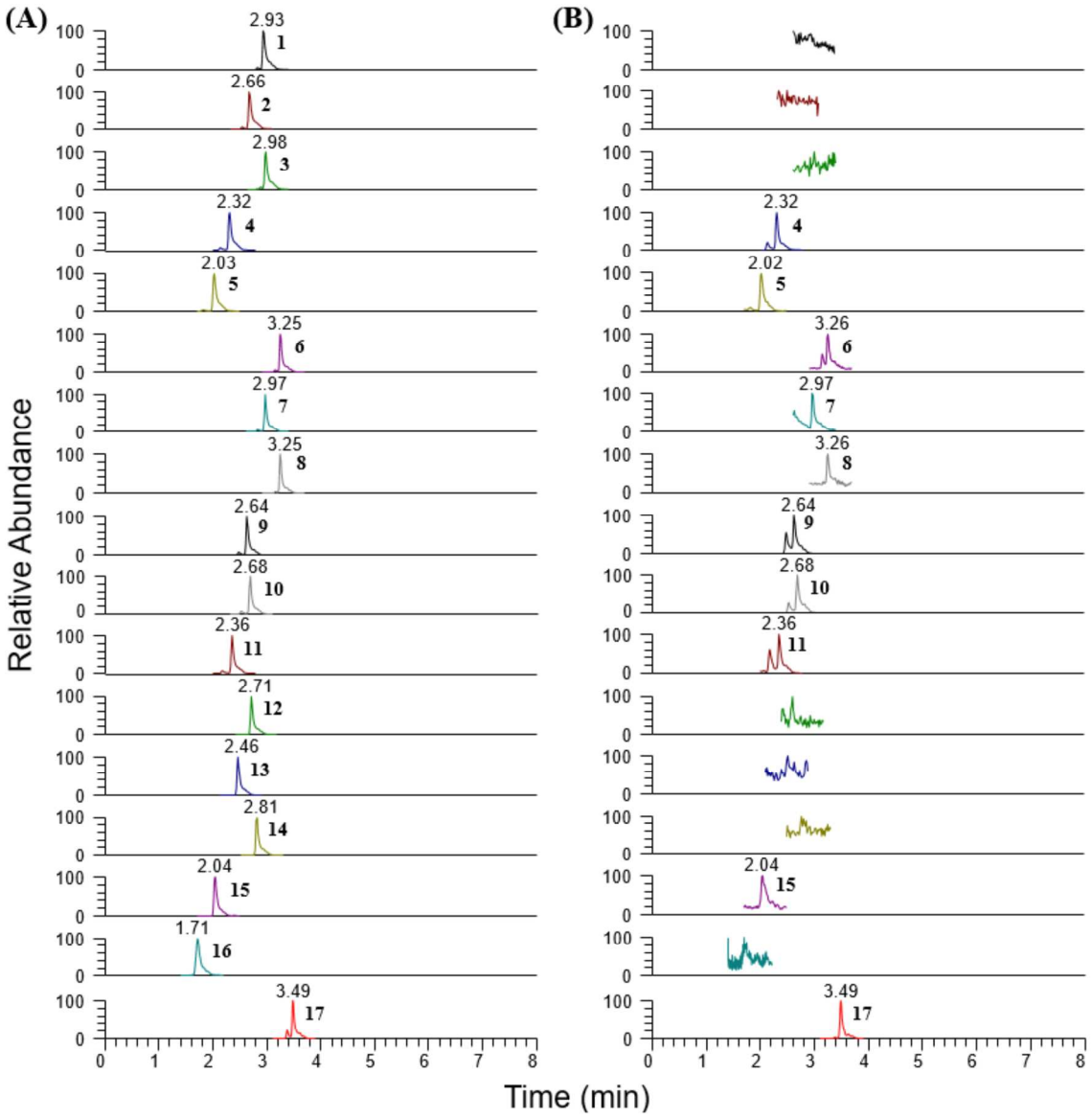
(A)
(B)
Relative Abundance
Time (min)
2.93 1
2.66 2
2.98 3
2.32 4
2.03 5
3.25 6
2.97 7
3.25 8
2.64 9
2.68 10
2.36 11
2.71 12
2.46 13
2.81 14
2.04 15
1.71 16
3.49 17
2.02 5
3.26 6
3.26 8
2.36 11
2.04 15

Figure 2.

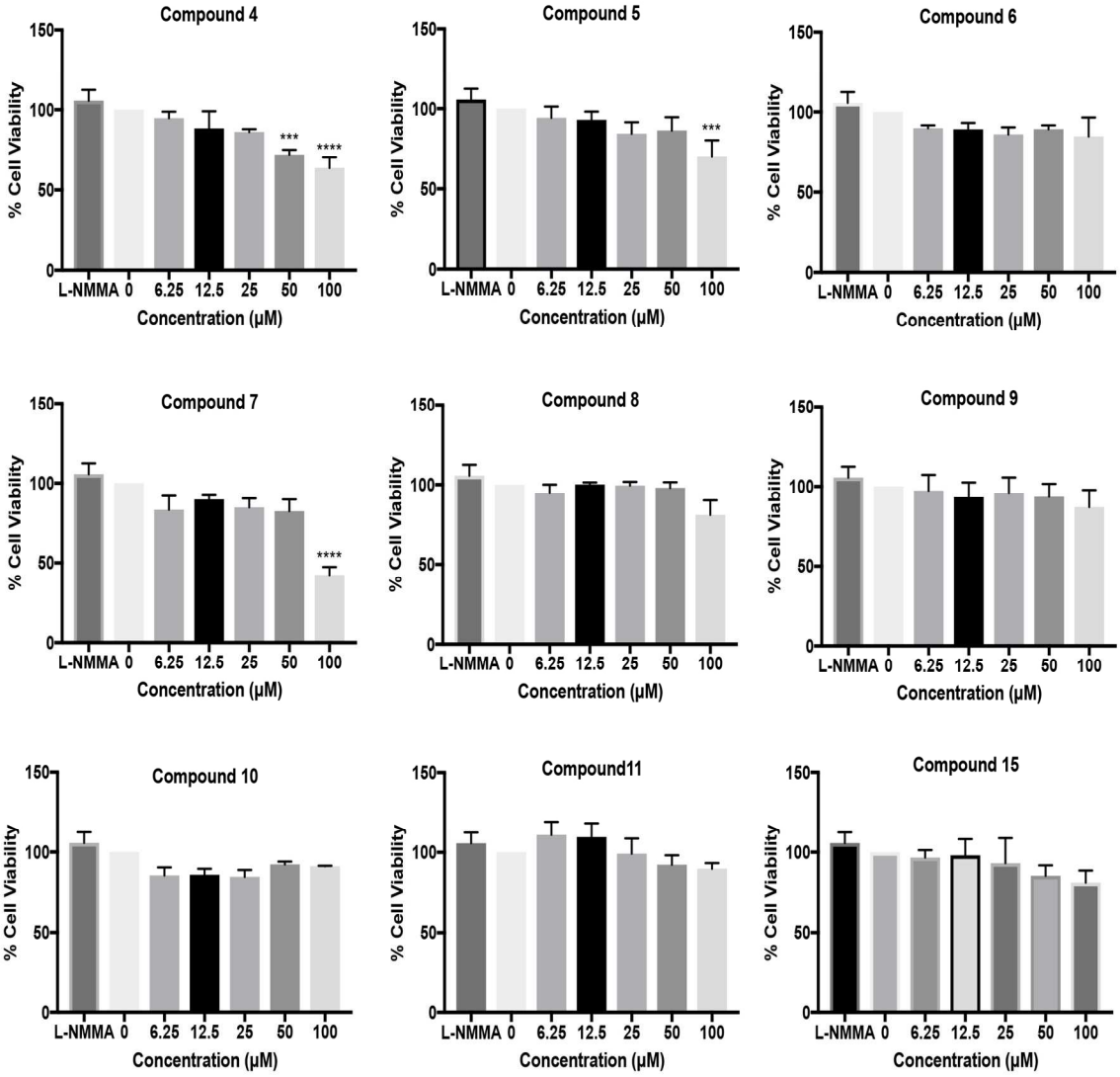
Compound 4
Compound 5
Compound 6
Compound 7
Compound 8
Compound 9
Compound 10
Compound11
Compound 15
% Cell Viability
150
100
50
0
L-NMMA 0 6.25 12.5 25 50 100
Concentration (μM)
***
****

Figure 3.

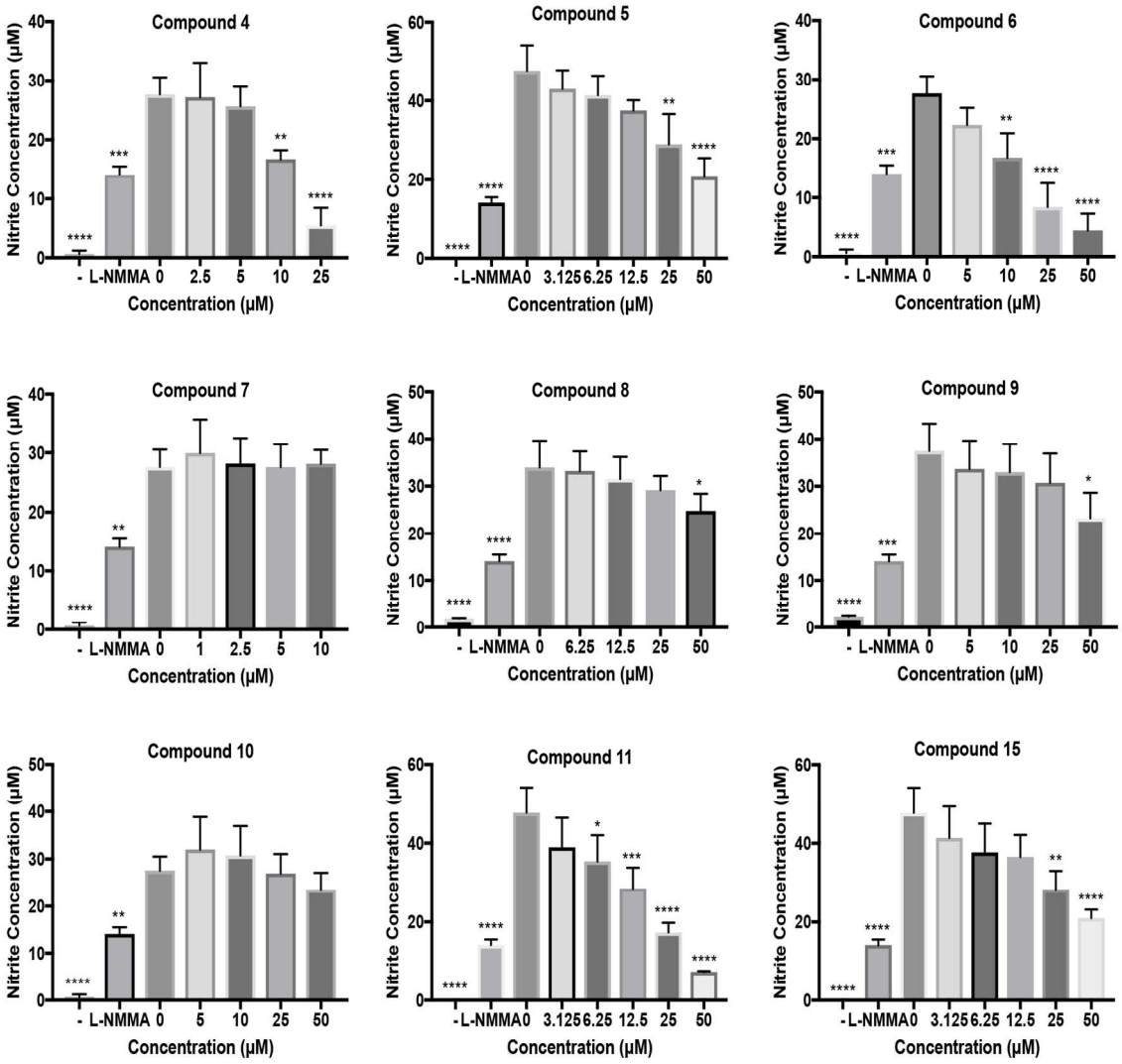
Compound 4
Nitrite Concentration (μM)
- L-NMMA 0 2.5 5 10 25
Concentration (μM)
Compound 5
Nitrite Concentration (μM)
- L-NMMA 0 3.125 6.25 12.5 25 50
Concentration (μM)
Compound 6
Nitrite Concentration (μM)
- L-NMMA 0 5 10 25 50
Concentration (μM)
Compound 7
Nitrite Concentration (μM)
- L-NMMA 0 1 2.5 5 10
Concentration (μM)
Compound 8
Nitrite Concentration (μM)
- L-NMMA 0 6.25 12.5 25 50
Concentration (μM)
Compound 9
Nitrite Concentration (μM)
- L-NMMA 0 5 10 25 50
Concentration (μM)
Compound 10
Nitrite Concentration (μM)
- L-NMMA 0 5 10 25 50
Concentration (μM)
Compound 11
Nitrite Concentration (μM)
- L-NMMA 0 3.125 6.25 12.5 25 50
Concentration (μM)
Compound 15
Nitrite Concentration (μM)
- L-NMMA 0 3.125 6.25 12.5 25 50
Concentration (μM)

Figure 4.

585

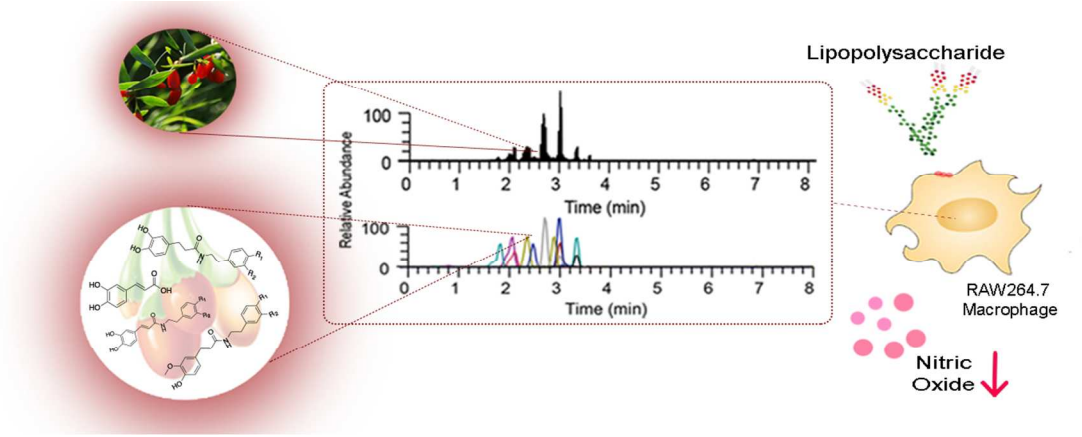

Table of Contents Graphic